Original Article

Surface pretreatment and cement influence on bond strength of three-dimensional printed permanent restorations

André Moreira[1,2,3], Bruno Areias[3,4], Sónia Simões[3,4], Miguel Pais Clemente[3,5], Pedro Sousa Gomes[1,2], Joaquim Mendes[3,4]

[1]BoneLab, Faculty of Dental Medicine, University of Porto, [2]LAQV/REQUIMTE, Faculty of Dental Medicine, University of Porto, [3]INEGI, Institute of Science and Innovation in Mechanical and Industrial Engineering, [4]Department of Mechanical Engineering, Faculty of Engineering, University of Porto, [5]Department of Surgery and Physiology, Faculty of Medicine, University of Porto, Porto, Portugal

Abstract

Context: Indirect permanent restorations re-establish strength, aesthetics, and function in compromised teeth. Three-dimensional (3D) printing has expanded to permanent restorations. Cementation and surface pretreatment critically influence adhesion and longevity, yet optimal protocols for 3D-printed restorations remain insufficiently established.

Aims: Evaluate the influence of surface pretreatment, cement type, and their combined effects on tensile bond strength (TBS), surface topography, and roughness of a definitive 3D-printed resin.

Materials and Methods: One hundred and eighty cubic specimens were 3D-printed with VarseoSmile Crown Plus. For surface pretreatment analysis, specimens were bonded with adhesive resin cement (ARC) after one of four protocols: No pretreatment (Control), Al_2O_3 airborne-particle abrasion (Air), diamond bur instrumentation (Bur), or polishing (Polished). Surface morphology and roughness parameters (Sq, Sp, Sv, Sz, and Sa) were characterized by digital microscopy and a scanning electron microscope. For cement type comparison, additional groups were prepared using Bur pretreatment combined with ARC, self-adhesive resin cement (SaRC), or resin-modified glass ionomer cement (RmGIC). All bonded pairs (n = 15 per group) underwent macro-tensile testing in a universal testing machine at a crosshead speed of 1 mm/min.

Statistical Analysis: One-way ANOVA was conducted. Bonferroni *post hoc* testing was performed for pairwise comparisons, with a significance level set at α =0.05 for all tests.

Results: TBS was significantly influenced by pretreatment ($P < 0.001$), with Bur producing the highest values and Polished the lowest (44.47 ± 37.24); no differences were observed among Control (180.53 ± 101.77), Air (155.92 ± 54.17), and Bur (238.87 ± 68.62). Surface analysis revealed significant differences only for Sv ($P = 0.023$), while Sq, Sp, Sz, and Sa remained comparable ($P > 0.05$). Cement type strongly affected TBS ($P < 0.001$), with ARC + silane achieving the highest values (238.87 ± 68.62), followed by SaRC (105.93 ± 20.70) and RmGIC (19.53 ± 18.61).

Conclusions: Cement type influenced critically on the TBS of the 3D permanent restoration; ARC protocols incorporating silane offered superior outcomes. None of the surface pretreatment protocols enhanced significantly TBS, and minimally influenced surface roughness.

Keywords: Adhesives; composite resins; dental cements; dental materials; three-dimensional printing

Address for correspondence:
Dr. André Moreira,
Faculty of Dental Medicine, University of Porto, Rua Dr. Manuel Pereira da Silva, Porto, 4200-393, Porto, Portugal.
E-mail: andre.luis.sa.moreira@gmail.com

Date of submission : 27.12.2025
Review completed : 07.01.2026
Date of acceptance : 13.01.2026
Published : 02.02.2026

Access this article online

Quick Response Code:

Website: https://journals.lww.com/jcde

DOI: 10.4103/JCDE.JCDE_1096_25

This is an open access article distributed under the terms of the Creative Commons Attribution-NonCommercial-NoDerivatives 4.0 License (CC BY-NC-ND), where it is permissible to download and share the work provided it is properly cited. The work cannot be changed in any way or used commercially without permission from the journal.

For reprints contact: WKHLRPMedknow_reprints@wolterskluwer.com

How to cite this article: Moreira A, Areias B, Simões S, Clemente MP, Gomes PS, Mendes J. Surface pretreatment and cement influence on bond strength of three-dimensional printed permanent restorations. J Conserv Dent Endod 2026;29:210-6.

INTRODUCTION

Indirect permanent restorations hold significant importance as a restorative solution for severely decayed or structurally compromised teeth, restoring biomechanical strength, improving aesthetics, and enhancing overall oral function.[1] Additive manufacturing – commonly referred to as three-dimensional (3D) printing – has emerged as a transformative approach. Initially introduced as stereolithography in the early 1980s, 3D printing has rapidly expanded in dentistry, enabling the fabrication of anatomical and prosthetic models, tissue engineering and regenerative scaffolds, surgical guides, occlusal devices, and a variety of other customized applications. More recently, the use of 3D printing for permanent restorations has gained increasing attention.[2,3]

The long-term success of permanent restorations depends on multiple factors, with the cementation method being one of the most critical. Effective cementation ensures durable retention and a reliable seal between the tooth and the restoration, minimizing the risk of microleakage and debonding over time.[4] Optimizing adhesion typically requires modifying surface topography to increase micromechanical retention, alongside the use of bonding agents to facilitate chemical interaction.[5,6] The choice of proper surface conditioning protocol is essential for the success of both ceramic and resin-based restorations across various dental applications.[7-9] Cement type is another determinant of bonding success. Performance variations are well documented across chairside CAD-CAM ceramics.[10] Thus, the selection of an appropriate luting agent depends on multiple factors, including the type of restorative material, surface pretreatment, and clinical scenario. However, in the case of 3D-printed permanent restorations, evidence is still limited regarding the ideal combination of surface pretreatment and cementation protocol to maximize bond strength and long-term clinical performance.

Accordingly, the present study aims to evaluate the bonding performance of resin-based restorations fabricated through 3D printing under different surface pretreatment conditions and cement types. To test these factors, the following null hypotheses were formulated:

H_{01}: There are no significant differences in macro-tensile bond strength (TBS) among 3D-printed resin specimens pretreated with airborne-particle abrasion using Al_2O_3, diamond bur, polishing, or no surface modification (control).

H_{02}: There are no significant differences in surface topography among 3D-printed resin specimens pretreated with airborne-particle abrasion using Al_2O_3, diamond bur, polishing, or no surface modification (control).

H_{03}: There are no significant differences in macro-TBS when 3D-printed resin specimens are cemented with an adhesive light-cure resin cement, a self-adhesive resin cement, or a resin-modified glass ionomer cement.

MATERIALS AND METHODS

A total of 180 cubic specimens (8 x 8 x 8 mm) were fabricated using a SprintRay Pro S printer with VarseoSmile Crown^{plus} resin (VSC+) (from BEGO), a material indicated by the manufacturer for permanent single-tooth restorations such as full crowns, inlays, onlays, and veneers. After printing, the specimens underwent an initial wash in 95% ethanol for 3 min, and a second wash in fresh 95% ethanol using an ultrasonic cleaner for 5 min. The specimens were then dried with oil-free compressed air and polymerized for 4 min in the ProCure Two (SprintRay) curing unit. The specimens were not polished or coated with any glaze to preserve the original printed surface for testing. All materials tested, their classification, brand name, and ref/lot number are mentioned in Supplementary Table 1.

This study did not require ethical approval, as it was an *in vitro* laboratory investigation using commercially available materials and did not involve human participants, human tissues, animals, or identifiable personal data.

The 180 specimens were randomly distributed among six groups ($n = 30$ per group). Since each pair of specimens was bonded together, the effective sample size per group was $n = 15$ bonded pairs.

Four groups were used to evaluate the effect of different surface pretreatments while employing the same adhesive light-cure resin cement (Variolink® Esthetic LC, Ivoclar):

- Control group (no pretreatment): No mechanical or chemical surface modifications were applied
- Air group (Al_2O_3 airborne-particle abrasion): Pretreatment with 50 µm (270 mesh) Al_2O_3 particles at 1.5 bar pressure (Zeta Sand, Zhermack)
- Bur group (Diamond bur): Pretreatment using a cylindrical high-speed diamond bur (KOMET, 2837. FG.014), followed by 5 s oil-free air drying
- Polished group: Pretreatment with sequential medium (gray) (KOMET, 9641M.HP. 100) and fine (yellow) (KOMET, 9644F.HP. 100) acrylic Polishedishers, each for 20 s, followed by 20 s of felt buffing (KOMET, 9628.HP. 220), and 5 s of oil-free air drying.

For these four groups, the following standardized bonding protocol was performed:

1. Application of silane (Ceramic Bond, VOCO) for 60 s, followed by gentle air drying with oil-free air for five seconds

2. Application of universal dental adhesive (Futurabond U *SingleDoce*, VOCO), followed by gentle air drying with oil-free air for five seconds
3. Application of adhesive light-cure resin cement (Variolink® Esthetic LC, Ivoclar)
4. Bonding of two specimens under gentle manual pressure, followed by UV light application for 20 s on each surface.

To evaluate the effect of cement type, three additional groups were prepared, while maintaining the same surface pretreatment, in this case, the diamond bur (Bur group) protocol:

- Adhesive light-curing resin cement (ARC): Upon the treatment of the surfaces, silane (Ceramic Bond, VOCO) was applied and allowed to react for 60 s, followed by gentle air drying with oil-free air for 5 s. Subsequently, a universal dental adhesive (Futurabond U *SingleDoce*, VOCO) was applied and air-dried using oil-free air for 5 s. The application of adhesive light-cure resin cement (Variolink® Esthetic LC, Ivoclar) and the specimens were bonded under gentle manual pressing. UV light curing was performed for 20 s per surface
- Self-adhesive resin cement (SaRC): Upon the treatment of the surfaces, a SaRC (Relix Unicem 2, 3M™) was applied, and specimens were manually pressed together. UV light curing was applied for 20 s on each surface
- Resin-modified glass ionomer cement (RmGIC): Upon the treatment of the surfaces, a resin-modified glass ionomer luting cement (GC FujiCEM™2, GC) was applied, and the specimens were pressed gently together for 4 min, as recommended by the manufacturer.

A schematic figure of the described protocol and specimens can be found in the appendix of this manuscript as Supplementary Figure 1.

Each bonded specimen was securely mounted into a universal testing machine (MultiTest 10-*i*, Mecmesin, Germany) [Supplementary Figure 2]. A uniaxial tensile load was applied perpendicular to the bonded interface at a crosshead speed of 1 mm/min until failure occurred. The obtained stress-strain data were analyzed using the Emperor (Force) software v1.18 - 408, West Sussex, United Kingdom. The peak load at failure was determined and converted into TBS. The failure modes were subsequently examined and classified according to the type of debonding.

Surface morphology and roughness were characterized using a Leica DM6 digital microscope at ×2000. Both brightfield and darkfield illumination modes were employed to enhance surface contrast, allowing for a detailed assessment of topographical features. 3D surface reconstructions were performed using the focus variation technique integrated into the system, enabling the quantification of surface roughness parameters. The acquired images and roughness profiles were analyzed using LAS X software (version 4.13.0), Leica Microsystems, Carnaxide, Portugal.

The morphological characteristics and elemental composition of representative samples from the four surface pretreatments were analyzed using a Thermo Scientific Phenom XL scanning electron microscope (SEM) equipped with an energy dispersive X-ray spectroscopy (EDS) detector. Samples were mounted on aluminum supports with a conductive carbon sheet. SEM images were obtained under low-vacuum conditions with an accelerating voltage of 15 kV. Elemental composition and distribution were assessed by EDS through spectra acquisition and elemental mapping.

All specimens were prepared following identical protocols regarding substrate selection, surface conditioning, adhesive application, and testing. Dimensions of specimens, preparation geometry, and curing parameters were strictly controlled to reduce variability related to sample preparation. Specimens were randomly allocated to each experimental group using a predetermined randomization sequence. This prevented selection bias and ensured that inherent variability in substrate characteristics was evenly distributed among groups. The operator performing the mechanical testing was blinded to group assignment to avoid measurement bias. In addition, coding of specimens during preparation and testing was used to maintain blinding. To avoid performance bias, all procedures were carried out under standardized environmental conditions (temperature, humidity, and storage). Mechanical testing was performed using the same testing machine, calibration settings, and loading rate for all groups. All materials used were from the same batch to avoid inter-batch variations. Manufacturers' instructions were followed precisely to reduce procedural bias. Only specimens meeting strict criteria for integrity, absence of cracks, and appropriate substrate quality were included. Exclusions were performed based on predefined criteria, not on group assignment or expected outcomes. Sample size was determined to ensure adequate power for detecting differences among groups with a software program (G*Power, ver. 3.1.9.7; Heinrich Heine Universität Düsseldorf). Effect size f 0.4, α err prob 0.05, Power ($1-\beta$ err prob) 0.8, number of groups 6, total sample size 90, actual power 0.823.

Data were collected and statistically analyzed using the SPSS Statistics version 27 software, IBM Inc., New York, EUA. Descriptive statistics were obtained. Normality and homogeneity of variance were confirmed prior to analysis. To evaluate the effects of surface pretreatment and cement type on TBS (H_{01} and H_{03}), one-way ANOVA was conducted. Bonferroni *post hoc* testing was performed for pairwise comparisons, with a significance level set at $\alpha = 0.05$ for all tests. For the roughness parameters comparison (H_{02}), when homogeneity of variance was not met (Levene's test, $P < 0.05$), a nonparametric Kruskal–Wallis test was used. A Chi-square test was conducted to assess the distribution of failure modes.

RESULTS

The uniaxial TBS test showed significant differences among the surface pretreatment groups bonded using the same adhesive light-cure resin cement. The Bur group exhibited the highest mean TBS, while the Polished group showed the lowest values. Statistical analysis revealed that only the Polished group was significantly different from all other groups ($F(3, 56) = 20.532$, $P < 0.001$), whereas no significant differences were observed among the Control, Air, and Bur groups. Detailed descriptive statistics are presented in Table 1, and a graphical comparison of group means with corresponding statistical outcomes is presented in Supplementary Figure 3.

Figure 1 shows representative 3D digital microscopy images of the surface morphology of the four pretreatment groups. Clear differences in surface texture and topography were observed, with color gradients indicating height variation – warmer colors (red/yellow) representing elevated regions and cooler colors (blue/green) representing depressions. The roughness characteristics and surface textures varied significantly between groups, reflecting the influence of each pretreatment method. The control group evidenced a more textured and irregular surface, characterized by ridges and depressions, resulting from the layering effect inherent to the 3D printing process. The air group presented a relatively uniform surface with a raised central region, possibly indicating localized deposition of the Al_2O_3 particles. The bur group showed linear striations along the surface, consistent with diamond bur instrumentation and producing a distinct anisotropic roughness. Polished group showed a smooth and undulating surface, typical of polishing-induced morphology.

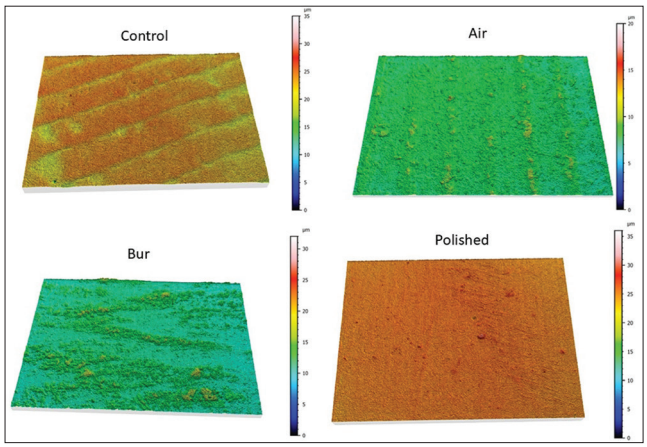

Figure 1: Representative three-dimensional digital microscopy images of the surface morphology from the different pretreatment groups. Images were obtained with ×2000. Color gradients represent surface height variations, with warmer tones (red/yellow) indicating elevated regions and cooler tones (blue/green) indicating depressions

The highest Sq and Sa values were found within the Bur group, whereas the lowest were observed in the Air and Polished groups. Relatively to Sp, Sv, and Sz, the highest values were found for the Polished group. Statistical analysis confirmed that all variables met the assumption of homogeneity of variances, and significant differences were identified only for Sv ($P < 0.05$ Air ≠ Polished). Supplementary Table 2 reports the mean and standard deviation for each roughness parameter (Sq, Sp, Sv, Sz, and Sa) per group and the multi-comparison result (*P* value). The SEM and EDS analyses [Figure 2] provide complementary insights into the microstructural and compositional changes induced by the different surface pretreatment protocols. The corresponding EDS map revealed a consistent elemental composition across the surface, predominantly showing carbon, oxygen, and silicon-reflective of the base resin matrix with minimal surface alteration [Supplementary Table 4].

To assess the influence of cement type on bonding performance, three groups were tested using the same surface treatment (Bur) but with different bonding

Table 1: Descriptive statistics of tensile bond strength for each surface pretreatment group, including mean peak force (N), mean peak stress (MPa), standard deviation, standard error, and minimum/maximum values

	n	Mean force (N)/ stress (MPa)	SD Force (N)/ stress (MPa)	SE force (N)/ stress (MPa)	Maximum force (N)/ stress (MPa)	Minimum force (N)/ stress (MPa)
Control	15	180.53/2.82	101.77/1.59	26.28/0.41	388/6.06	74/1.16
Air	15	155.92/2.44	54.17/0.85	13.99/0.22	260/4.06	62/0.97
Bur	15	238.87/3.73	68.62/1.07	17.72/0.28	367/5.73	104/1.63
Polished	15	44.47/0.69	37.24/0.58	9.61/0.15	134/2.09	2/0.03

SD: Standard deviation, SE: Standard error

Table 2: Descriptive statistics of tensile bond strength values for different cement types

	n	Mean force (N)/ stress (MPa)	SD force (N)/ stress (Mpa)	SE force (N)/ stress (MPa)	Maximum force (N)/ stress (Mpa)	Minimum force (N)/ stress (MPa)
ARC	15	238.87/3.73	68.62/1.07	17.72/0.27	367/5.70	104/1.16
SaRC	15	105.93/1.66	20.70/0.32	5.35/0.08	141/2.20	67/1.05
RmGIC	15	19.53/0.31	18.61/0.29	4.81/0.08	55/0.86	0/0

Values include mean peak force (N) and mean peak stress (MPa), along with SD, SE, and minimum/maximum values (n=15 per group). ARC: Adhesive resin cement, SaRC: Self-adhesive resin cement, RmGIC: Resin-modified glass ionomer cement, SD: Standard deviation, SE: Standard error

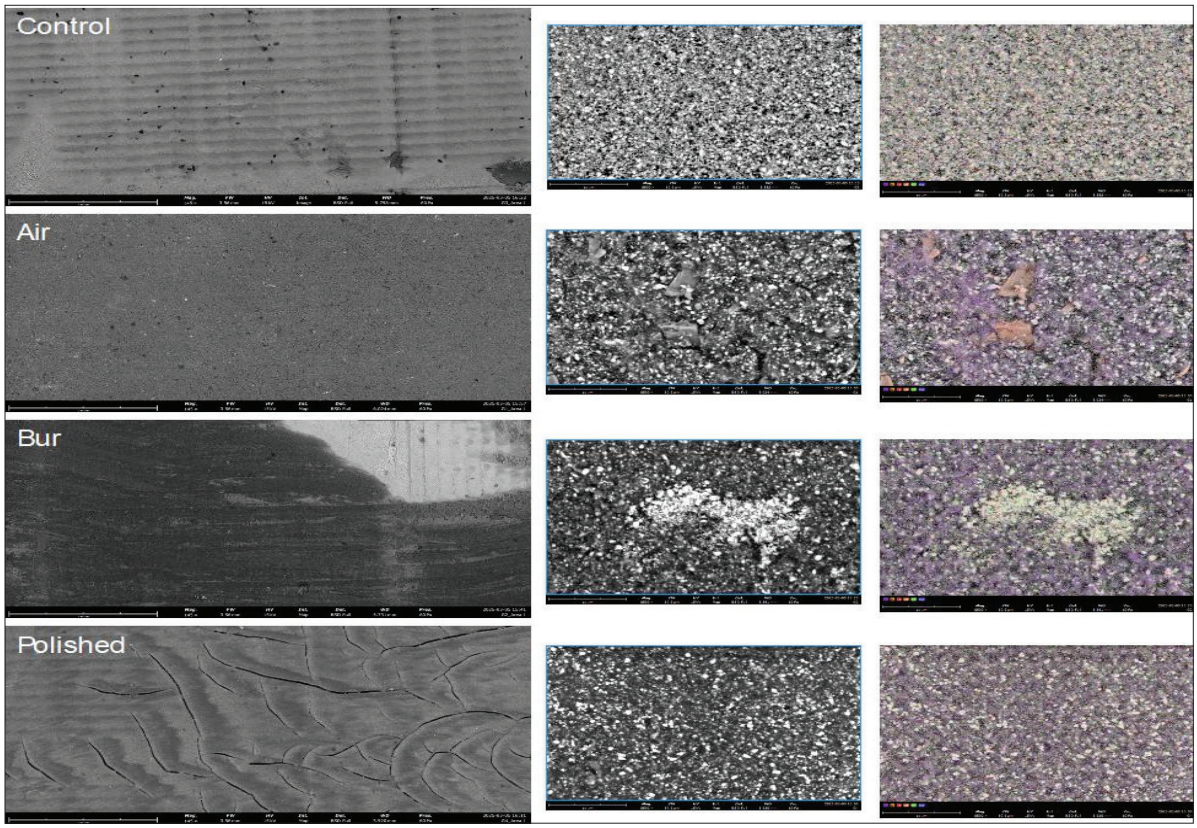

Figure 2: Representative scanning electron microscope images and corresponding energy dispersive X-ray spectroscopy elemental maps of the different surfaces of pretreatment groups, illustrating morphological features and compositional distributions

protocols: ARC, SaRC, and RmGIC. Among the three, the ARC group showed the highest TBS values. In comparison, the SaRC group showed significantly lower TBS, and the RmGIC group presented the lowest mean values. Descriptive statistics, including the mean peak force and stress, along with their respective standard deviation and error, are provided in Table 2. When testing null hypothesis 3, statistical analysis revealed a significant effect of cement type ($F(2, 42) = 100.163$, $P < 0.001$). Bonferroni-adjusted pairwise comparisons confirmed statistically significant differences among all groups ($P < 0.001$). A graphical comparison of group means with corresponding statistical outcomes is presented in Supplementary Figure 4.

Failure mode distribution for the pretreatment group is summarized in Supplementary Table 3 – Section A. When considering the Bur pretreatment combined with different cements [Supplementary Table 3 – Section B], distinct patterns were observed. Chi-square tests confirmed that the ARC group differed significantly from both SaRC and RmGIC. Representative post-TBS test specimens are presented in Supplementary Figure 5.

DISCUSSION

With the growing use of 3D-printed permanent restorative materials, understanding the factors that influence their clinical performance has become essential. Among these, surface pretreatment, cement type, and their combined effect on bond strength, surface roughness, and morphology play a critical role in ensuring restoration durability. The present study sought to address these gaps by systematically evaluating TBS alongside surface and cementation variables.

The first null hypothesis was rejected. Statistically significant differences were found for TBS among the four surface pretreatments applied to the same 3D-printable permanent resin bonded with a single adhesive protocol. The statistically significant differences found were strongly related to the presence of the Polished group. The Polished group recorded the lowest and was significantly different from all other groups. The Bur group achieved the highest TBS, although no significant differences were observed among the Air, Bur, and Control groups. These *in vitro* findings suggest that conditioning the intaglio surface of a 3D-printed crown with a rotary bur may enhance bonding, comparable to no pretreatment or Al_2O_3 airborne-particle abrasion; whereas polishing may compromise cementation outcomes. To the best of our knowledge, few studies have reported TBS of definitive 3D-printed permanent resins. Existing literature has focused mainly on provisional 3D-printed resins, typically evaluated through shear bond strength tests, which differ

methodologically from the pull-off tensile approach used in the present study. Although not directly comparable, such reports provide useful context since shear bond strength values are generally higher-approximated those of TBS, with engineering data suggesting a ratio of up to 2.4:1.[11] Within this framework, Lim and Shin report that although air-abrasion with Al_2O_3 created micro-retentive features in a provisional 3D-printed resin, there was no significant improvement in shear bond strength compared with the control.[12] Similarly, Ersöz *et al*. reported no significant differences between control, air-abraded, and hydrofluoric acid-treated groups in two permanent 3D-printed resins.[13] Kang *et al*. also found no significant differences between air-abrasion and control, although they reported a slight improvement when combined with a universal adhesive.[14] Graf *et al*. compared bonding properties of a definitive 3D-printed resin to milled composites and found that airborne-particle abrasion had no significant effect on pull-off strength, consistent with our findings that the Air and Control groups behaved similarly.[15]

To complement the bond strength analysis, surface characterization was conducted through digital microscopy and SEM. At ×2000 magnification, digital microscopy revealed that Sq and Sa were lower for Air and Polished groups, whereas the Bur group presented higher values, in agreement with the superior TBS observed for this group. No significant differences were found among groups for Sq, Sp, and Sz or Sa, while Sv values differed significantly, reflecting variations in maximum pit depth. Accordingly, the second null hypothesis was mostly accepted, as only for the parameter Sv statistically significant differences were found among groups. Regardless, the enhanced performance of the Bur group may be explained by the ability of rotary instrumentation to create deeper, more defined grooves and striations, which increase surface area and promote effective micromechanical retention. In addition, bur abrasion may expose filler particles within the resin matrix, potentially improving chemical interactions with silane and resin cement. By contrast, air-abrasion in this material appears to function more as a smoothing rather than a roughening step, while polishing reduced the surface energy and roughness, both of which may compromise bonding. Furthermore, the surface roughness (Sa) values are consistent with ranges reported in previous studies (0.06–39.00 μm).[16]

Regarding the influence of cement type, the third null hypothesis was also rejected. Statistically significant differences were found between the three cements, demonstrating that cement type significantly affected the TBS of specimens made from the same 3D-printable permanent resin pretreated with a high-speed diamond bur. Among them, the ARC (Variolink Esthetic LC) showed the highest bond strength, outperforming both the SaRC (RelyX Unicem) and the resin-modified glass ionomer cement (Fujicem 2). Comparable findings were reported for 3D-printable provisional resins, as reported by Holmer *et al*., who found that Variolink® Esthetic showed a higher bond strength compared to Fuji Cem 2.[17] Additional insight is provided by Lim *et al*., who suggested that joint copolymerization between residual monomers on the 3D-printed resins and resin cement monomers may enhance adhesion. Their research presented results corroborating that micromechanical treatments on 3D-printed provisional resins did not significantly increase shear bond strength, but cementation protocols including silane improved outcomes.[12] In the present study, SaRC and RmGIC, which were bonded without silane, were outperformed by ARC which incorporated silane in the adhesive protocol.

When analyzing the failure modes during the TBS test, one should have in consideration that the cement was bonded to two similar substrates. This likely explains the low incidence of adhesive failures, since such failures are more common when bonding dissimilar substrates, where the adhesive may have a stronger-chemical and/or mechanical interaction with one surface than the other. In the present study, most groups exhibited predominantly cohesive failures, indicating that fracture typically occurred within the cement itself rather than at the interface. This pattern was consistent across groups, except for the Bur pretreatment bonded with the ARC group, where substrate failure was predominant. This occurrence suggests that the bond strength between resin cement and restoration exceeded the internal cohesive strength of the 3D-printed resin, in line with the highest TBS values recorded. These failures were characterized by delamination along the printed layers, pointing to material-dependent limitations rather than an adhesive weakness. Interestingly, the Polished pretreatment cemented with the ARC group showed the lowest TBS, and presented the highest frequency of adhesive failures, reinforcing the notion of compromised interfacial bonding after polishing.

Despite the rigorous experimental design and standardized protocols employed, several limitations of this *in vitro* study should be acknowledged when interpreting the results. First, this investigation was conducted under *in vitro* conditions, which do not fully replicate the complex oral environment. Factors such as thermal fluctuations, masticatory fatigue, saliva composition, pH changes, enzymatic activity, and biofilm formation were not simulated. The absence of thermocycling, mechanical aging, or long-term water storage limits the extrapolation of the findings to clinical longevity and bond durability over time. Second, only one 3D printing resin (VSC+) and one printing system were evaluated. Differences in resin chemistry, filler content, degree of conversion, and printing technologies (e.g., DLP vs. LCD vs. SLA) may influence surface characteristics and bonding behavior. Therefore, the results cannot be generalized to all 3D-printed dental

resins. Third, specimens were fabricated as simple cubic blocks with flat bonding surfaces, which do not fully represent the geometry, fit variation, and stress distribution found in clinical restorations and tooth preparations, such as crowns, inlays, or onlays. The stress patterns generated during tensile testing differ from the complex multiaxial stresses encountered intraorally. Fourth, bond strength was assessed exclusively using a uniaxial TBS test. While tensile testing allows standardized comparison between groups, it does not reflect the combined shear, tensile, and compressive forces acting on restorations *in vivo*. Additionally, bond strength values are influenced by the substrate that the restoration is bonded (enamel, dentin, restorative material). Despite these limitations, the present study provides clinically relevant comparative data on the influence of surface pretreatment strategies and cement type on the bond strength of 3D-printed dental resins, contributing valuable insights for optimizing adhesive protocols in the rapidly expanding field of additively manufactured restorative materials.

CONCLUSIONS

H01 was rejected.

- The type of surface pretreatment significantly affected TBS ($P < 0.001$)
- Diamond bur pretreatment yielded the highest mean TBS values
- No significant differences were observed among the control, Al_2O_3 air-abrasion, and diamond bur groups
- Polishing significantly reduced TBS and showed the lowest values.

H02 was mostly accepted.

- Significant differences were observed only for Sv ($P = 0.023$)
- No significant differences were found for Sq, Sp, Sz, or Sa ($P > 0.05$).

H03 was rejected.

- The cement type/protocol significantly influenced TBS ($P < 0.001$)
- ARC with silane showed the highest TBS values
- SaRC showed intermediate performance
- Resin-modified glass ionomer cement resulted in the lowest TBS.

Overall, the present results highlight that cement type and adhesive protocol may exert a stronger influence on bonding performance than the surface pretreatment strategy.

Data availability statement

Authors will provide the database upon request.

Acknowledgments

The authors would like to thank VOCO and BEGO for supporting the investigation with their dental materials. The authors would like to thank Dr. José Pedro Dias da Silva for sharing his printing machine to produce all samples.

Financial support and sponsorship

This work received no direct funding. The coauthor, Pedro S.Gomes received support and help from FCT/MCTES (LA/P/0008/2020 -DOI 10.54499/LA/P/0008/2020, UIDP/50006/2020 -DOI 10.54499/UIDP/50006/2020, UIDB/50006/2020 -DOI 10.54499/UIDB/50006/2020), through national funds.

Conflicts of interest

There are no conflicts of interest.

REFERENCES

1. Sequeira-Byron P, Fedorowicz Z, Carter B, Nasser M, Alrowaili EF. Single crowns versus conventional fillings for the restoration of root-filled teeth. Cochrane Database Syst Rev 2015;2015:CD009109.
2. Gross BC, Erkal JL, Lockwood SY, Chen C, Spence DM. Evaluation of 3D printing and its potential impact on biotechnology and the chemical sciences. Anal Chem 2014;86:3240-53.
3. Schweiger J, Edelhoff D, Güth JF. 3D printing in digital prosthetic dentistry: An overview of recent developments in additive manufacturing. J Clin Med 2021;10:2010.
4. Edelhoff D, Ozcan M. To what extent does the longevity of fixed dental prostheses depend on the function of the cement? Working Group 4 materials: cementation. Clin Oral Implants Res 2007;18 Suppl 3:193-204.
5. Ghodsi S, Shekarian M, Aghamohseni MM, Rasaeipour S, Arzani S. Resin cement selection for different types of fixed partial coverage restorations: A narrative systematic review. Clin Exp Dent Res 2023;9:1096-111.
6. Moura DM, Veríssimo AH, Leite Vila-Nova TE, Calderon PS, Özcan M, Assunção Souza RO. Which surface treatment promotes higher bond strength for the repair of resin nanoceramics and polymer-infiltrated ceramics? A systematic review and meta-analysis. J Prosthet Dent 2022;128:139-49.
7. Matinlinna JP, Lung CY, Tsoi JK. Silane adhesion mechanism in dental applications and surface treatments: A review. Dent Mater 2018;34:13-28.
8. Akgungor G, Sen D, Aydin M. Influence of different surface treatments on the short-term bond strength and durability between a zirconia post and a composite resin core material. J Prosthet Dent 2008;99:388-99.
9. Bouschlicher MR, Cobb DS, Vargas MA. Effect of two abrasive systems on resin bonding to laboratory-processed indirect resin composite restorations. J Esthet Dent 1999;11:185-96.
10. Ustun S, Ayaz EA. Effect of different cement systems and aging on the bond strength of chairside CAD-CAM ceramics. J Prosthet Dent 2021;125:334-9.
11. Silfwerbrand J. Shear bond strength in repaired concrete structures. Mater Struct 2003; 36:419-24.
12. Lim NK, Shin SY. Bonding of conventional provisional resin to 3D printed resin: The role of surface treatments and type of repair resins. J Adv Prosthodont 2020;12:322-8.
13. Ersöz B, Aydın N, Ezmek B, Karaoğlanoğlu S, Çal İK. Effect of surface treatments applied to 3D printed permanent resins on shear bond strength. J Clin Exp Dent 2024;16:e1059-66.
14. Kang YJ, Park Y, Shin Y, Kim JH. Effect of adhesion conditions on the shear bond strength of 3D printing resins after thermocycling used for definitive prosthesis. Polymers (Basel) 2023;15:1390.
15. Graf T, Erdelt KJ, Güth JF, Edelhoff D, Schubert O, Schweiger J. Influence of pre-treatment and artificial aging on the retention of 3D-printed permanent composite crowns. Biomedicines 2022;10:2186.
16. Moreira A, Gomes PS, Clemente MP, Mendes J. Comparative evaluation of 3D-printed resins for single-tooth dental crowns – Provisional and permanent: A scoping review. Eur J Prosthodont Restor Dent 2025;33:296-317.
17. Holmer L, Othman A, Lührs AK, von See C. Comparison of the shear bond strength of 3D printed temporary bridges materials, on different types of resin cements and surface treatment. J Clin Exp Dent 2019;11:e367-72.

Supplementary Table 1: Material tested, classification, brand name, and reference/lot number

Classification	Commercial product (trade name, manufacturer)	Reference/lot
3D printing resin	VarseoSmile Crown Plus, BEGO	Ref 41118 Lot 601572
Adhesive resin cement	Variolink Esthetic LC, Ivoclar	Ref 763424WW Lot Z077FX
Self-adhesive resin cement	Relyx Unicem 2, 3 M	REF 56847 LOT 11319132
Resin-modified glass ionomer luting cement	Fujicem 2, GC	Ref 900897 Lot 230726A
Silane	Ceramic Bond, VOCO	Ref 1106 LOT 2436485
Universal adhesive	Futurabond U (singledose), VOCO	Ref 1572 LOT 2411222

3D: Three-dimensional

Supplementary Table 2: Roughness parameters for each pretreatment group

Roughness parameter (μm)	Control	Air	Bur	Polished	*P*
Sq	1.05±0.131	0.72±0.117	1.76±0.588	0.74±0.086	0.093
Sp	5.96±0.727	10.03±1.218	14.42±4.404	21.30±12.658	0.436
Sv	14.32±2.917	11.18±2.082	14.80±2.081	23.67±3.452	0.023
Sz	20.27±2.951	21.21±2.738	29.23±5.842	31.78±4.309	0.159
Sa	0.78±0.790	0.54±0.090	1.26±0.410	0.51±0.068	0.082

Values are reported as mean±SD. Sq (RMS height), Sp (Max peak height), Sv (Max pit depth), Sz (Max height), Sa (Arithmetical mean height). SD: Standard deviation

Supplementary Table 3: Distribution of failure types: Section A for each surface pretreatment group bonded with adhesive resin cement; Section B: For Bur-pretreated samples bonded with different cements

Section A	Air	Bur	Control	Polished
Adhesive	1	0	3	5
Cohesive	10	1	8	10
Substrate	4	13	2	0
Mixed (substrate + cohesive/adhesive)	0	1	2	0
n	15	15	15	15

Section B	ARC	SaRC	RmGIC
Adhesive	0	0	0
Cohesive	1	13	15
Substrate	13	1	0
Mixed (substrate + cohesive/adhesive)	1	1	0
n	15	15	15

ARC: Adhesive resin cement, SaRC: Self-adhesive resin cement, RmGIC: Resin-modified glass ionomer cement

Supplementary Table 4: Element name and percentage according to pretreatment group

Element name	Control	Air	Bur	Polished
Carbon	21.81	58.83	58.47	54.83
Nitrogen	3.36	2.16	-	2.50
Oxygen	50.93	30.53	33.98	35.23
Aluminum	3.39	2.18	1.06	1.54
Silicon	16.41	5.10	5.30	5.90
Barium	4.10	1.19	1.19	1.00

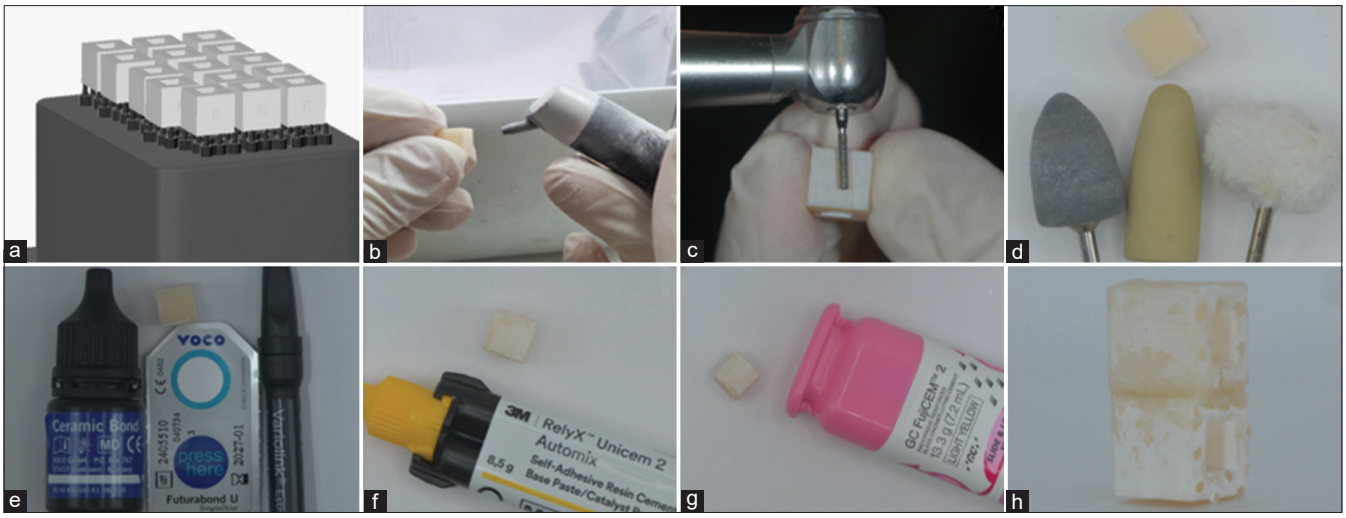

Supplementary Figure 1: Panel of figures representing the methodology. (a) STLs of the specimens prepared in the printing software of SprintrayCloud; (b) Airborne-particle abrasion with Al_2O_3 (Air group); (c) Roughening with a high-speed diamond bur (Bur group); (d) Set of acrylic polishers used for the Polished group; (e) Materials used for the ARC group; (f) Cement used for the SaRC group; (g) Cement used for RmGIC; (h) One bonded paired-specimen before the TBS test, each group had 15 pairs

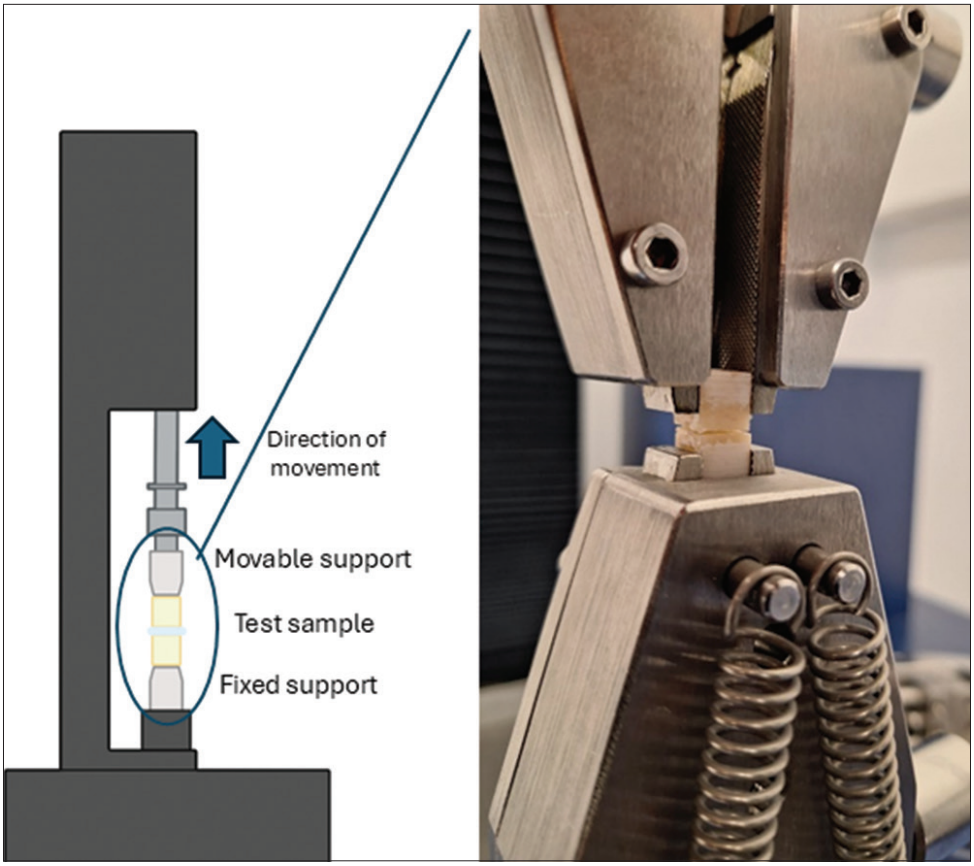

Supplementary Figure 2: Schematic diagram (left) and corresponding photograph (right) of the macro-tensile bond strength test setup. The bonded resin specimens were clamped between the fixed lower support and the movable upper shaft of the universal testing machine, MultiTest 10-i, ensuring uniaxial tensile loading perpendicular to the bonding interface

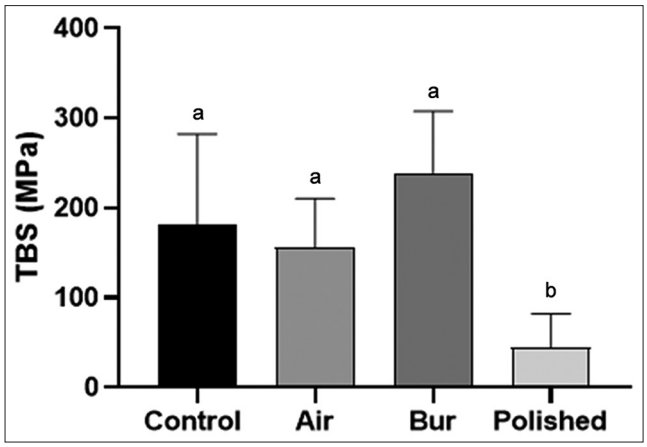

Supplementary Figure 3: Mean tensile bond strength for each surface pretreatment group. Different lowercase letters indicate significant differences, $P < 0.001$. ($n = 15$ per group). "a" identifies statistically similar groups. "b" identifies the group with statistically significances during Bonferroni *post hoc* multiple comparisons

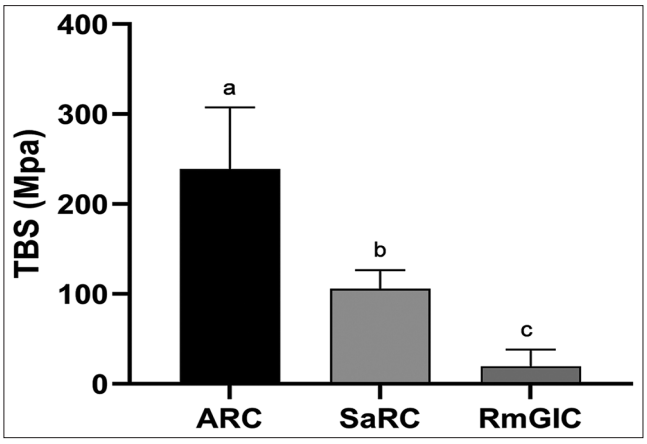

Supplementary Figure 4: Mean tensile bond strength for each cement type. Different lowercase letters indicate significant differences, $P < 0.001$. ($n = 15$ per group). "a", "b", and "c" represent that all groups had statistically significant differences during Bonferroni *post hoc* multiple comparisons

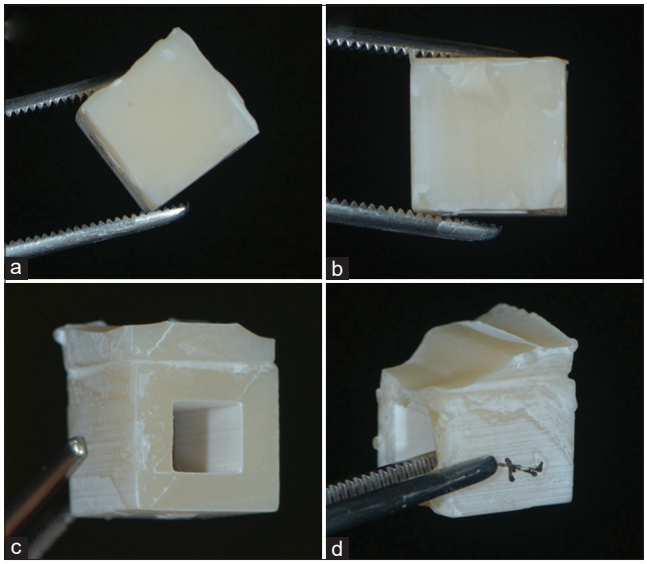

Supplementary Figure 5: Representative post tensile bond strength test specimens depicting the main failure pattern: (a) adhesive failure; (b) cohesive failure; (c) substrate failure; and (d) mixed failure (combination of substrate, cohesive, and/or adhesive failure)